

# Microwave Breast Tumor Detecting and Targeting Employing Multiswarm Contrast-Agent-Loaded Bacterial Nano robots

Pagadala Sree Harsha<sup>1</sup>, Divya. K , B. Jaiganesh<sup>2</sup>

Dept. of ECE, Saveetha School of Engineering, Saveetha University, Tiruvallur, Tamilnadu, India

**Abstract**—The orders and speeds of bio-compatible flagellated magneto tactic bacteria (MTB) might be accompanied alongside pre-planned trails deep inside the human body across external magnetic fields. Furthermore, a microwave difference agent such as carbon nanotubes (CNTs) could be loaded onto MTB to change the dielectric properties of tissues adjacent the agent. Instituted on these two phenomena, we illustrate how several aggregations of MTB released into human breast can be pursued simultaneously and monitored using the differential microwave imaging (DMI) technique. We also present novel strategies to detect and localize a breast cancerous mass across the DMI-trackable bacterial propulsion and steering period, and use an anatomically realistic breast ideal as a tested to confirm the feasibility of this breast cancer diagnostic method.

**Keywords:** flagellated magneto tactic bacteria (MTB), carbon nanotubes (CNTs), differential microwave imaging (DMI) technique.

## I. INTRODUCTION

Microwave breast imaging aims at differentiating breast tissues based on their dielectric properties, which are sensitive to physiological or pathological factors of clinical interest. Nevertheless, the efficacy of this modality is significantly affected by strong interference due to normal tissue heterogeneities. This challenge could be overcome by using a contrast medium such as carbon nanotubes (CNTs) to alter the dielectric properties of a tumor. These agents can be delivered selectively to the cancer via systemic administration for noninvasive and specific identification of regions of interest. However, only a low volumetric concentration of contrast agents is able to reach cancer cells by using currently available targeting techniques. Recent progress in Nano robotics has promised a possible remedy for this problem through the prospect of realizing bio-compatible flagellated miniature robots combined with the nanometer-sized magnetisms of magneto tactic bacteria (MTB), whose directions and displacement speeds can be controlled by an external magnetic field. Furthermore, the MTB can be

used to transport contrast agents efficiently to a tumor location in deep regions of human body. The strategy for MTB-assisted microwave breast tumor sensing and targeting was first proposed in [1], where each time a single swarm of MTB loaded with a Nano composite contrast agent was injected into the human breast. The MTB will align in the direction of an external magnetic field and its motion can be tracked by using the differential microwave imaging (DMI) technique proposed. When a particular swarm trajectory meets a tumor, the contrast agent will be unloaded and bound to cancer cell receptors. Once unloaded, the swarm will no longer be visible by DMI, which only tracks difference in the tissue microwave properties due to the agent. Thus, the site where the contrast agent eventually accumulates will correspond to an MTB footprint “sink” inside breast. The current work extends the results in [1] by considering multiple aggregations of MTB, which are administered simultaneously into the breast at each round of injection to reduce the sensing time. The DMI algorithm in [1] can only estimate the location of the nearest swarm. As a result, antennas can be divided into several groups. Each group tracks the associated nearest agglomeration of MTB. By applying the prior knowledge of magnetic fields created, and imposing the constraint that MTB positions must be aligned with magnetic fields, the average speed of electromagnetic wave in breast can be approximated and the bacterial swarms are tracked. The feasibility of the proposed solution is studied by using an anatomically realistic breast model from the University of Wisconsin Computational Electromagnetics (UWCEM) Lab’s breast phantom repository [2].

## II. STRATEGY FOR BREAST TUMOR DETECTION AND LOCALIZATION

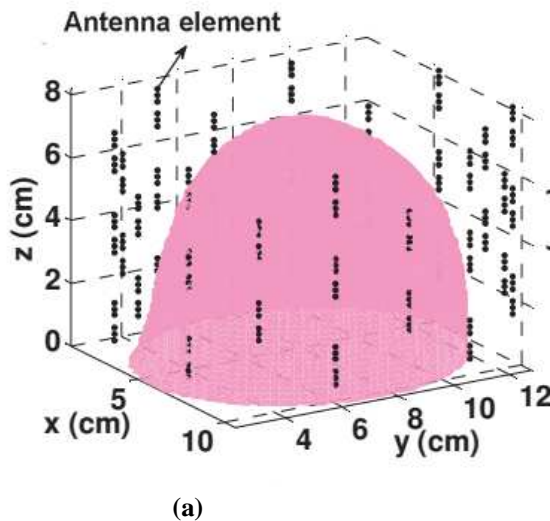


Fig. 1: (a) Illustration of the tumor detecting arrangement employing a configuration comparable

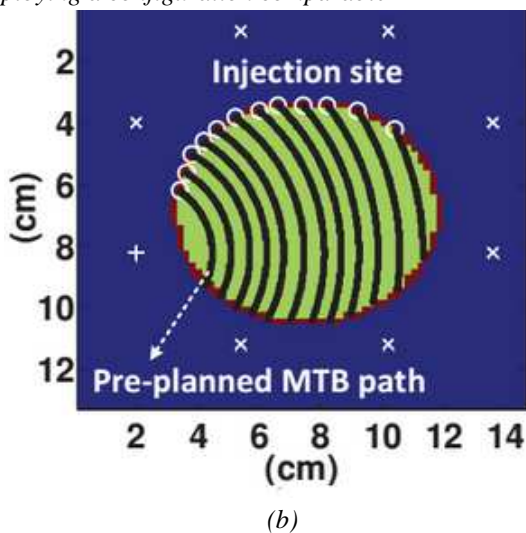


Fig.1: (b) Dielectric profile at 1 GHz for the coronal cross-section across the third antenna ring. We accept concentric magnetic earth lines initiating from a dc basis via one of the antennas (marked alongside a '+') across the propulsion-and-steering phase. All eight antennas probe the breast sequentially alongside ultra-wideband pulses across the pursuing phase. Two clumps of MTB are released simultaneously into the breast.

To illuminate our strategies, we ponder a "heterogeneously dense" breast phantom from the UWCEM repository, encompassing one tumor having the median properties of malignant glandular breast tissue. We retain the a like 40-element dipole array configuration as in that is coordinated above five cylindrical rings shown in Figure 1(a). Our aim in this discovers is to present two-dimensional (2-D) detecting and diagnosis alongside each of the cross-sectional planes of the rings employing three-dimensional (3-D) data. As an example, we ponder the cross-sectional plane of the third ring from

the top, that passes across the tumor and has a dielectric profile shown in Figure 1(b). We will merely use monocratic data from the eight antennas of the third ring to elucidate our detecting algorithm, even though a fully 3-D multistate DMI way is additionally possible. The attendance of a difference medium in or adjacent a tissue span will considerably change its innate dielectric properties. Consider that flagellated MC1-MTB are loaded alongside a microwave agent and released simultaneously into human body from two distinct inoculation locations as illustrated in Figure 1(b). An external basis creates a magnetic earth by way of a wire allocated close to the biological object below examination that determines the association in that the MTB will align. We spread the DMI algorithm counseled in to several targets as to be debated in Serving 3. This method is next utilized to trail the gestures of these two agglomerations of Nano robots in usual intervals by noticing and localizing the change in tissue dielectric properties in their proximal regions. If a swarm of bacteria flounder to sense a tumor (i.e., the corresponding MTB trail does not intersect the tumor), the swarm will retain traversing in capillary channels in the orders aligned to the magnetic earth lines till being accompanied out of human body. On the supplementary hand, if the swarm detects a tumor, the difference medium will be unloaded and attached to cancer cell receptors. After unloaded, this swarm will no longer be visible by DMI that merely tracks contrasts in tissue microwave properties due to the agent. Thus, the locale whereas the difference agent in the end accumulates will correspond to a "sink" alongside the pre-planned MTB trajectory. Several tissue anomalies will lead to several MTB footmarks "sinks". Tumors can be therefore noticed via this seeing-is-sensing principle. The frank sequence of events is methodical as follows.

**Initialization:** Prior to the inoculation procedure, we sequentially send ultra-wideband radar pulses from every single antenna agent to probe the breast as shown in Figure 1(b), and record the backscatter reply at every single element. These data in the nonexistence of difference agent will be utilized as the baseline data in the DMI procedure at a afterward stage.

**Propulsion and steering:** We design the MTB trails in the breast established on its geometry and ascertain the inoculation locations on the breast surface. This survey design should safeguard that the whole breast inside is obscured alongside sufficiently tiny gaps amid bordering paths to cut fake negatives. We next infuse several clusters of contrast-agent-attached MTB into the breast, and escort them alongside a magnetic earth for a enumerated era  $t_{ps}$ . We accept that the result of the magnetic earth is to escort the swarms alongside

concentric magnetic gradients generated at one of the eight antennas as exemplified in Figure 1(b).

**Tracking:** We switch the arrangement setting from the propulsion-and-steering mode to the pursuing mode. The early pace is to send sequentially the alike waveform as the one utilized in the initialization period from every single antenna agent and record the corresponding backscatter response. Apply the spread DMI algorithm to be debated in Serving 3 to trail several swarms for area of  $t_T$ . The period  $t_T$  ought to be retained as short as probable to minimize the random diffusion of Nano robots in the nonexistence of a steady manipulating magnetic force. On the supplementary hand,  $t_T$  ought to be long plenty to permit adequate buy of backscatter data for precise pursuing of MTB. In exercise, a  $t_T$  in an order of a insufficient seconds should be adequate for the pursuing intention (noting that actual processing of the gesture might be gave in the subsequent propulsion-and-steering cycle).

**Decision-making:** We next choose whether the tumor detecting procedure is finished, given the MTB tracks and subject to a sequence of criteria: (i) Are the agglomerations of MTB yet in the breast? (ii) Has a DMI impression “sink” been observed? (iii) Have all the pre-planned trails been completed? If the answer is “yes” to all of them, we state that tissue malignancies have been prosperously noticed and localized. Otherwise, the arrangement could discharge new agglomerations of MTB or the aged ones can tolerate maneuvering, reliant on whether the early populaces are yet present in the breast.

### III. TRACKING OF MULTIPLE AGGREGATIONS OF MTB

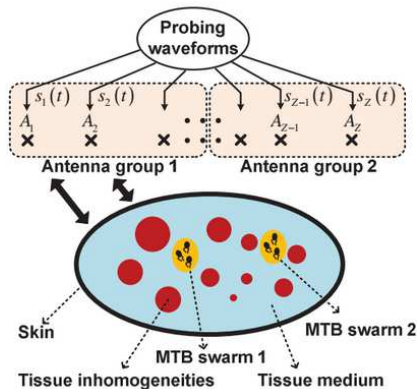


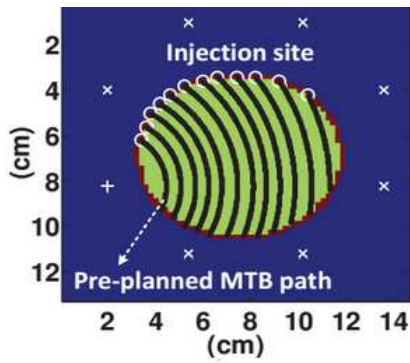
Fig. 2: An interference-prone breast channel whereas two agent- loaded MTB swarms are present in the unkempt breast alongside tissue in homogeneities.

In this serving we spread the DMI algorithm counseled in to notice several innate dielectric adjustments provoked by countless agglomerations of contrast-agent-attached MTB. Lacking defeat of generality, we ponder an interference-prone breast medium as shown in Figure 2,

whereas two swarms of bacteria are present in a unkempt biological medium generated by healthy breast tissue heterogeneities. Think a radar arrangement encompassing several spatially varied monocratic antenna agents,  $A_1, A_2, \dots, A_Z$ . Every single antenna embodies both a gesture basis allocated an mechanical earth and an observation sensor. We will use the subscript  $z$  in the pursuing discussion to indicate the parameters associated alongside antenna  $A_z$  ( $z = 1, 2, \dots, Z$ ). Presume that the stay taps gave by the two clusters of agent-loaded MTB at  $A_z$  are  $1,z$  and  $2,z$ . Attendance of difference agent in the breast will distort the biological channel reply provoked by adjustments in the tissue dielectric properties. We note that merely the late reply alongside larger stay than  $z = \min\{1,z, 2,z\}$  will be influenced. Subsequently, we can tear all antenna agents into two clusters as shown in Figure 2. For every single associate fitting in to antenna cluster  $k$  ( $k = 1, 2$ ),  $z = k, z$ . In this method, every single cluster merely monitors the alike nearest MTB swarm. Therefore, we can apply undeviatingly the DMI algorithm, that is suitable for single-target detection and localization, to compute the time-of-arrival (TOA)  $z$ . If the MTB trails are projected such that the two swarms should be well separated in the breast at each period instant, we can present effortlessly antenna gathering given the locations of the dc basis and infusion sites. The data mixture method counseled in merges the TOA measurements from disparate antennas to attain an guesstimate of the target location. This method though needs vision of the average tissue dielectric properties, that cannot be obtained in a realistic clinical setting. The counseled tumor detecting way provides an interesting resolution to the above setback by approximating simultaneously the mean propagation speed of signals and the swarm location. We accept that an antenna  $A_z$  is pursuing the  $k_{th}$  MTB swarm.  $A_z$  is placed at  $(x_z, y_z)$  and measures a TOA  $\tau_z = zT_0$ , whereas  $T_0$  is the sampling time. The TOA  $\tau_z$  defines a circle concentrated at  $A_z$  alongside radius  $r_z = v_{\tau_z}/2$  whereas  $v$  is the average speed of electromagnetic wave in the breast and is connected to the mean tissue permittivity and conductivity. We find the locale of the  $k_{th}$  MTB swarm by minimizing the sum of square of the distances from the swarm to the points of intersection of the scope circles closest to it. Given an average speed of waves  $v$ , an optimum no iterative resolution  $x_{k(v)}$  of the locale of the  $k_{th}$  swarm can be obtained pursuing . Next, we impose the constraint that MTB impressions ought to be aligned alongside the hypothetical circular magnetic field lines alongside radius  $R$  generated by a dc basis placed at  $x_{dc}$ . Consequently, the average speed  $v$  is approximated to  $v^* = \text{argmin}_v[|x_k(v) - x_{dc}| - R]$  and the corresponding swarm footmark is given

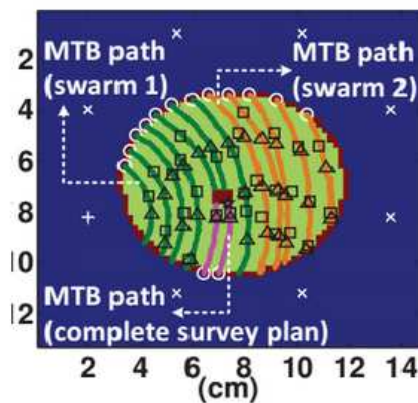
by  $x_k(v^*)$ .

IV. SIMULATION RESULTS



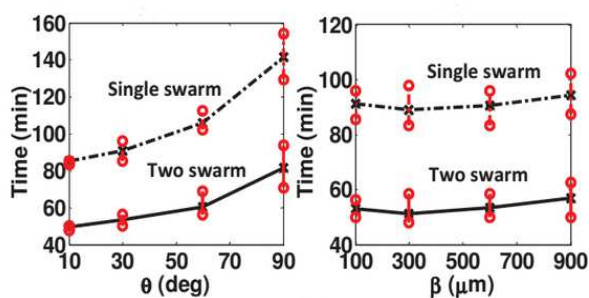
(a)

Fig. 3: (a) Pre-planned MTB trails for the arrangement setup in Figure 1



(b)

Fig. 3: Simulated DMI footprints. The MTB inoculation locations are marked alongside "o".



(c)

Fig. 3: (c) Detecting period versus angular range  $\theta$  and mean pace size  $\beta$  of the directional random walk for single- and two-swarm administration. The fixed parameter values are  $\beta = 100 \mu m$  in the preceding and  $\theta = 30^\circ$  in the latter.

We use numerical examples to elaborate on the tumor detecting strategy highlighted above. Our target is to simulate probable gestures of the swarms due to the consented magnetic earth and examination the DMI's

skill to trail their trajectories and sense the tumor. Figure 1 displays the layout of the health diagnostic arrangement as debated in Serving 2. The inoculation locations are consistently spaced on the external of the 2-D cross-sectional plane of the phantom delineated in Figure 1(b), that is additionally illustrated in Figure 3(a) (marked alongside circles). Figure 3(a) additionally illustrates the pre-planned MTB paths obscuring uniformly the finished breast interior; the distance amid two adjacent trails is concerning 5mm, that determines the resolution of this particular breast survey plan. Two MTB swarms are released into the breast at the alike period, whereas their infusion locations are spaced separately across the whole detecting procedure to safeguard prosperous pursuing as indicated in Serving 3. We accept that every single populace of MTB follows a directional random stroll across the propulsion-and-steering stage. Consequently, every single pace size of swarm varies according to an exponential allocation alongside a mean worth, and the association at every single pace is uniformly distributed amid  $[-, +]$ . Here is the mean association aligned alongside the tangent of the magnetic earth and measures the encounter of random directional disturbance provoked by supplementary gradients (chemo taxis and aero taxis) and abnormal microvasculature networks. Finally, we accept that the MTB aggregations pursue an isotropic random stroll alongside the alike pace size allocation across the pursuing stage. The early speeds of both swarms prior to inoculation are selected as 200 m/s, and cut alongside period in the breast pursuing the consequence. The periods for the propulsion-and-steering and pursuing periods are  $t_{ps} = 2 \text{ min}$  and  $t_T = 5 \text{ s}$ , respectively. To simulate the encounter of every single CNTs-loaded MTB swarm on the dielectric properties of breast tissues, we ponder that CNTs change the dielectric benefits for one  $2 \times 2 \times 2 \text{ mm}^3$  cubic voxel concentrated at the point whereas the MTB swarm is present. We accept the comparative permittivity and conductivity of this voxel to be 22% and 70% higher than the median properties of malignant glandular breast tissue. This assumption is motivated by the result of CNTs on malignant tissue consented in . A normal simulated detecting procedure ( $\alpha = 30^\circ, \beta = 100 \mu m$ ) alongside the DMI impressions plotted is illustrated in Figure 3(b). Examples of the precise locations of MTB across the pursuing period are marked alongside triangles, and the corresponding approximated locations via DMI are marked alongside squares. Think two swarms released simultaneously from the 1st and the 8th infusion sites. These two populaces of MTB were accompanied by the magnetic fields to move for 2 min and grasped the early locations whereas the pursuing was performed. Later 5 s

of pursuing (noting that the displacement of MTB was nearly imperceptible in this case due to the short pursuing duration), the arrangement was switched back to the propulsion-and-steering mode, whereas the swarms endured maneuvering and the spread DMI algorithm gave in Serving 3 was requested to localize the MTB for the preceding pursuing cycle. This procedure was recapped periodically. After each of the two swarms left the breast, we released one more agglomeration of MTB from the inoculation locale subsequent to it, and so on. The finished good accord amid the precise and approximated locations of the MTB demonstrates the efficacy of the spread DMI method for pursuing the CNTs-loaded bacteria Nano robots. For well-planned swarm trajectories, a DMI impression "sink" indicating the tumor locale will be noted, as delineated in Serving 2. It is worth emphasizing that two supplementary MTB injections at the bottom of the breast phantom were given to finish the early survey design pictured in Figure 3(a). The benefits of the angular range and the mean pace size will alter the tumor detecting period and therefore the performance of the counseled method. The average period consumed in tumor detecting alongside alongside the maximum and minimum benefits for and is shown in Figure 3(c), suitably, for ten autonomous simulations of the MTB pursuing processes. Evidently, by employing two aggregations of MTB in parallel, momentous reduction in the period consumed in finishing the breast surveying is attained as contrasted to the single-swarm deployment. Furthermore, the detecting period mean and dispersion rise as the angular range increases, as the average detecting period and its dispersion are not altered by disparate values.

## V. CONCLUSION

This preliminary discover gave novel schemes for microwave breast cancer detection alongside the use of multiswarm bacterial Nano robots. Countless key assumptions have to be confirmed for these methods to be clinically feasible. These contain the efficiency of the MTB as manipulated trackable propulsion and steering arrangements, as well as the skill of our spread DMI algorithm to notice the MTB swarms established on the result of their difference agent cargos inside the tissue.

## REFERENCES

- [1] Karpowicz, N., H. Zhong, J. Xu, K. Lin, J. S. Hwang, and X. C. Zhang, "Comparison between pulsed terahertz imaging time-domain imaging and continuous wave terahertz imaging," *Semiconductor Science and Technology*, Vol. 20, No. 7, 293–299, Jul. 2005.
- [2] Smith, D., "Microwave holographic measuring method and apparatus," Patent Application, No. 0022503.7, UK, Sep. 2000.
- [3] Elsdon, M., D. Smith, M. Leach, and S. J. Foti, "Experimental investigation of breast tumor imaging using indirect microwave holography," *Microwave and Optical Technology Letters*, Vol. 48, No. 3, 480–482, Mar. 2006.
- [4] Arakaki, A., Webb, J., and Matsunaga, T. (2003) A novel protein tightly bound to bacterial magnetic particles in *Magnetospirillum magneticum* strain AMB-1. *J Biol Chem* **278**: 8745–8750.
- [5] Arakaki, A., Masuda, F., Amemiya, Y., Tanaka, T., and Matsunaga, T. (2010) Control of the morphology and size of magnetite particles with peptides mimicking the Mms6 protein from magnetotactic bacteria. *J Colloid Interface Sci* **343**: 65–70.
- [6] Bartlett, J.D., Ganss, B., Goldberg, M., Moradian-Oldak, J., Paine, M.L., Snead, M.L., et al. (2006) 3. Protein-protein interactions of the developing enamel matrix. *Curr Top Dev Biol* **74**: 57–115.
- [7] Bazylinski, D.A., and Frankel, R.B. (2004) Magnetosome formation in prokaryotes. *Nat Rev Microbiol* **2**: 217–230.
- [8] Ding, Y., Li, J., Liu, J., Yang, J., Jiang, W., Tian, J., et al. (2010) Deletion of the *ftsZ*-like gene results in the production of superparamagnetic magnetite magnetosomes in *Magnetospirillum gryphiswaldense*. *J Bacteriol* **192**: 1097–1105.
- [9] N. K. Nikolova, "Microwave imaging for breast cancer," *IEEE Microw. Mag.*, vol. 12, no. 7, pp. 78–94, 2011.
- [10] M. Lazebnik, D. Popovic, and et al., "A large-scale study of the ultrawideband microwave dielectric properties of normal, benign and malignant breast tissues obtained from cancer surgeries," *Phys. Med. Biol.*, vol. 52, pp. 6093–6115, 2007.
- [11] A. Mashal, B. Sitharaman, and et al., "Toward carbon-nanotube-based theranostic agents for microwave detection and treatment of breast cancer: Enhanced dielectric and heating response of tissue-mimicking materials," *IEEE Trans. Biomed. Eng.*, vol. 57, pp. 1831–1834, Aug. 2010.
- [12] S. Martel, M. Mohammadi, O. Felfoul, Z. Lu, and P. Pouponneau, "Flagellated magnetotactic bacteria as controlled MRI-trackable propulsion and steering systems for medical nanorobots operating in the human microvasculature," *Int. J. Rob. Res.*, vol. 28, pp. 571–582, Apr. 2009.